Contrib Mineral Petrol (2016) 171:76
DOI 10.1007/s00410-016-1282-4

ORIGINAL PAPER

Copper isotope behavior during extreme magma differentiation and degassing: a case study on Laacher See phonolite tephra (East Eifel, Germany)

Jian Huang[1] · Sheng-Ao Liu[2] · Gerhard Wörner[3] · Huimin Yu[1] · Yilin Xiao[1]

Received: 17 April 2016 / Accepted: 29 July 2016 / Published online: 18 August 2016

Abstract Copper (Cu) isotopic analyses were performed on a set of samples from the Laacher See tephra (LST) (Eifel, Germany) to investigate whether Cu isotopes are fractionated during extreme magma differentiation and degassing. The LST represents a continuous fractional crystallization series from parental basanite through mafic to highly differentiated phonolites. Samples analyzed here include phonolites of variable degrees of differentiation, phonolite–basanite hybrid rocks formed by mixing basanite and phonolite magmas, and basanite-derived mega-crystals (i.e., clinopyroxene, amphibole, phlogopite). In addition, we analyzed a series of mafic parental lavas from surrounding volcanic centers to constrain the Cu isotopic features of the Eifel mantle. Mafic phonolites show strong depletion in Cu compared to their parental basanites from ~50 to ~3 ppm, indicating sulfide fractionation during the basanite-to-phonolite differentiation. Mass balance calculations, based on the most Cu-rich hybrid rock ($\delta^{65}Cu = -0.21$ ‰, [Cu] = 46.2 ppm), show that the parental basanite magmas have $\delta^{65}Cu$ of ca. −0.21 ‰, lighter than those of the mafic phonolites (~0.11 ‰). This suggests that sulfide fractionation preferentially removes the lighter Cu isotope (^{63}Cu) in S-saturated magmas. By contrast, all phonolites have a limited range of Cu contents (1.1 to 4.0 ppm) with no systematic variations with S, suggesting that Cu is not controlled by sulfide fractionation during the evolution of mafic to highly differentiated phonolites. The identical $\delta^{65}Cu$ values (0.11 ± 0.03 ‰, 2SD, $n = 10$) of the phonolites, irrespective of highly diverse composition and extents of differentiation, indicate that fractional crystallization of silicates (e.g., plagioclase, sanidine, amphibole, pyroxene, olivine), Fe–Ti-oxides and phosphate (e.g., apatite) generates insignificant Cu isotope fractionation. The lack of correlations between $\delta^{65}Cu$ and volatile contents (e.g., S, Cl) in the LST sequence implies that volcanic degassing causes no detectable Cu isotope fractionation of igneous rocks. Eifel basalts and mega-crystals have variable $\delta^{65}Cu$ (−0.18 to 0.21 ‰) that are uncorrelated to MgO and Cu, suggesting that such variations were not caused by differentiation but reflect the Cu isotopic heterogeneity of the Eifel mantle source due to metasomatism by fluids derived from hydrothermally altered oceanic lithosphere.

Keywords Cu isotopes · Magma differentiation · Degassing · Laacher See volcano · Eifel basalt

Communicated by Jochen Hoefs.

✉ Jian Huang
jianhuang@ustc.edu.cn

✉ Sheng-Ao Liu
lsa@cugb.edu.cn

[1] CAS Key Laboratory of Crust-Mantle Materials and Environments, School of Earth and Space Sciences, University of Science and Technology of China, Hefei 230026, China

[2] State Key Laboratory of Geological Processes and Mineral Resources, China University of Geosciences, Beijing 100083, China

[3] Division of Geochemsitry, Geosciences Center, University of Göttingen, 37077 Göttingen, Germany

Introduction

Copper is a redox-sensitive transition metal element that has two stable isotopes of ^{65}Cu and ^{63}Cu with relative abundances of 69.17 and 30.83 %, respectively (Lodders 2003). With the advent of multiple collector inductively-coupled plasma mass spectrometry (MC-ICPMS), the

geochemistry, cosmochemistry, and biogeochemistry of Cu isotopes can be studied (e.g., Albarède 2004 and references therein). It has been widely accepted that Cu isotope ratios (expressed as $\delta^{65}Cu = (((^{65}Cu/^{63}Cu)_{sample}/(^{65}Cu/^{63}Cu)_{NIST\ 976} - 1) \times 1000)$ can be significantly fractionated during a variety of low-temperature processes, including (1) redox reactions (e.g., Zhu et al. 2002; Ehrlich et al. 2004; Fernandez and Borrok 2009; Pekala et al. 2011), (2) mineral dissolution and precipitation (e.g., Ehrlich et al. 2004; Mathur et al. 2009, 2010, 2012; Fernandez and Borrok 2009; Kimball et al. 2009; Wall et al. 2011), (3) sorption of aqueous Cu^{2+} onto mineral and bacterial surfaces (e.g., Mathur et al. 2005; Balistrieri et al. 2008; Bigalke et al. 2010; Little et al. 2014; Li et al. 2015), and (4) biological activity (e.g., Zhu et al. 2002; Weinstein et al. 2011; Jouvin et al. 2012).

However, whether or not a detectable Cu isotope fractionation occurs during high-temperature magmatic processes is an on-going debate. By studying primitive basalts, Savage et al. (2013) concluded that no resolvable Cu isotope fractionation occurs during mantle partial melting. This is supported by the indistinguishable $\delta^{65}Cu$ of mid-ocean ridge basalts (MORBs), ocean island basalts (OIBs), komatiites, and mantle peridotites (Liu et al. 2015a; Savage et al. 2015a), although partial melting is likely to fractionate Cu isotopes in some melt-depleted mantle xenoliths (Savage et al. 2014, 2015b). Li et al. (2009) concluded that granite magma differentiation produces insignificant Cu isotope fractionation based on the tight clustering of $\delta^{65}Cu$ (0.03 ± 0.15 ‰) for a suit of evolved I-type granites. In a conference abstract, Savage et al. (2015b) reported that Cu isotope fractionation during basalt magma differentiation depends on the oxygen fugacity of the system and the mineral phases crystallized. In S-undersaturated magmas, no detectable Cu isotope fractionation was observed, while in S-saturated magmas, minor, but resolvable Cu isotope fractionation occurred (Savage et al. 2015b). This suggests that sulfide fractionation plays a potential role in controlling Cu isotope fractionation during magma differentiation, because sulfide is enriched in the lighter Cu isotope (^{63}Cu) relative to coexisting silicates (Savage et al. 2015a), and this may have consequences in global geochemical differentiation processes.

A compilation of published data show that fresh igneous rocks, including basalts and granites, display variable $\delta^{65}Cu$ ranging from −0.46 to 0.49 ‰ (e.g., Archer and Vance 2004; Li et al. 2009; Bigalke et al. 2010; Liu et al. 2014a, b, 2015a), but the reasons for such variations are unknown. These Cu isotopic variations exceed about 20 times that of the current analytical precision (±0.05 ‰, e.g., Maréchal et al. 1999; Liu et al. 2014b) and may reflect either Cu isotope fractionation during high-temperature magmatic processes and/or source heterogeneity. Liu et al. (2015a) found that arc basalts from Kamchatka display variable $\delta^{65}Cu$ ranging from −0.19 to 0.47 ‰ and attributed such variations to the involvement of recycled crustal materials in their mantle source. However, it is unconvincing to apply Cu isotopes to reveal source heterogeneity of mantle-derived magmas and its cause unless the magnitude and direction of Cu isotope fractionation during magma differentiation and degassing are known (Maher et al. 2011). Theoretical studies have shown that magmatic vapor phases (e.g., Cu_3Cl_3) are enriched in heavier Cu isotopes relative to the melt phase where $[CuCl_3]^{2-}$ and $[Cu(HS)_2]^-$ compounds are present (Seo et al. 2007; Fujii et al. 2013, 2014). In contrast, experimental studies have indicated that vapor-hosted Cu is enriched in the lighter isotope (^{63}Cu) compared to that in liquids (Rempel et al. 2012). This discrepancy promotes fundamental questions: whether or not Cu isotope fractionation occurs during magma degassing and in what direction.

Here, we present high-precision Cu isotopic analyses for a set of well-characterized, differentiated phonolites from the Laacher See tephra (LST) (East Eifel, Germany) that were erupted 13 ka ago from a single vent and produced a voluminous (6.3 km^3) compositionally zoned tephra deposit. This volcano represents the youngest and most voluminous eruption in the Quaternary alkaline intra-plate East Eifel volcanic field. The LST reflects in its compositional zonation a cogenetic series from mafic to highly evolved phonolite with extreme depletion in MgO, Sr, and Ba and strong incompatible trace element enrichment (Wörner and Schmincke 1984a, b). This highly evolved phonolite cupola was fluid-saturated and actively degassing prior to eruption. The mafic parent to this differentiation series has been identified to be basanitic in composition (Wörner and Schmincke 1984b). These characteristics make the compositionally zoned Laacher See phonolite deposit and surrounding (older) mafic parental lavas an excellent natural laboratory to study elemental and isotopic behavior during magma differentiation and degassing. The main goal of this study is to investigate Cu isotope behavior during extreme magma differentiation from parental basanite through mafic to highly differentiated phonolites and associated magma degassing. In addition, we analyzed a range of basalts and mineral mega-crystals (i.e., clinopyroxene, amphibole, phlogopite) from the E and W Eifel to constrain the Cu isotopic characteristics of the sub-Eifel mantle. Basement rocks (i.e., slate, greywacke) and crustal xenoliths (i.e., mica-schist, granulite) were further studied to evaluate the effect of crustal contamination on the Cu isotopic composition during magmatic differentiation.

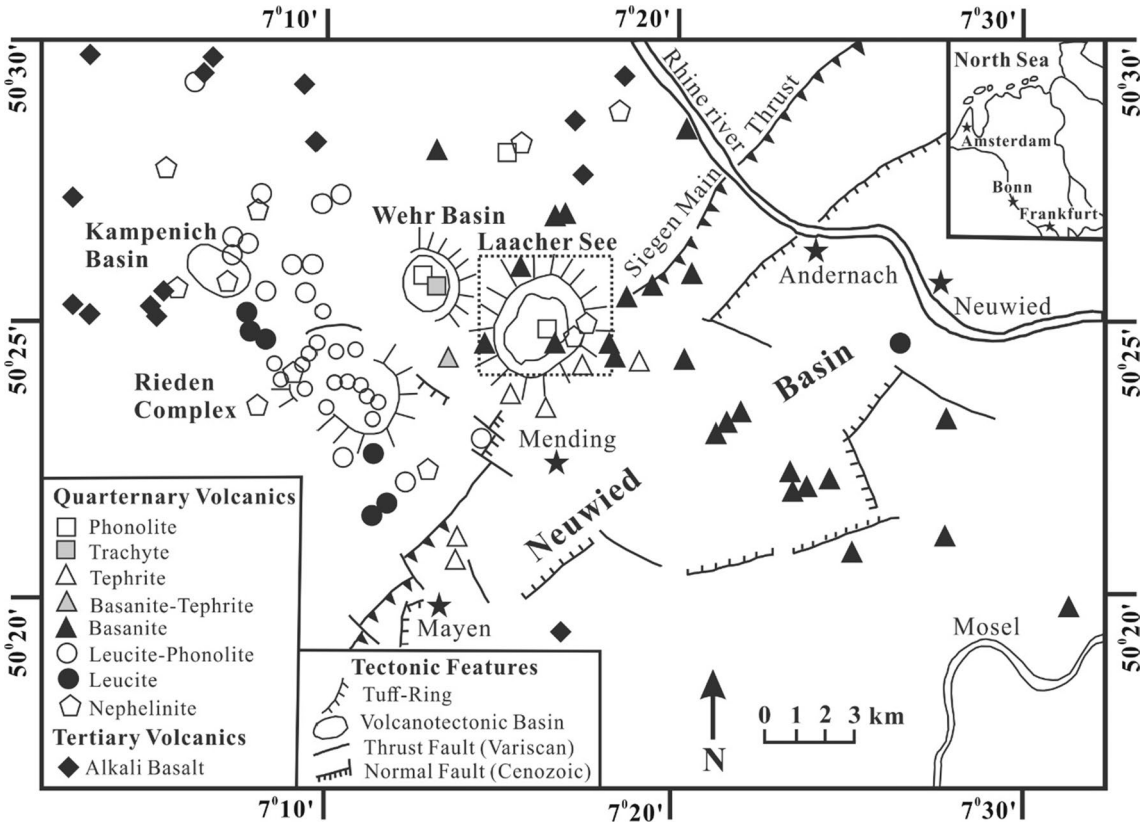

Fig. 1 The eruptive centers of the Quaternary East Eifel volcanic field with the Laacher See volcano emphasized by a large *dashed square.* Modified from Wörner et al. (1987)

Geological settings and sample descriptions

The East Eifel volcanic field

The Quaternary East Eifel Volcanic Field (EEVF) is located west of the Rhine River in the uplifted Paleozoic Rhenish Massif (Fig. 1). The locally exposed country rock consists of folded Devonian slates, sandstones, and graywackes as well as Tertiary sediments. Crustal xenoliths (e.g., mica schist, gneiss, migmatite, and granulite) are found in several Eifel volcanoes (Wörner et al. 1982; Wörner and Schmincke 1984a) and represent the older greenschist- and amphibolite-facies basement rocks underlying the Devonian strata.

Around 100 eruptive centres have been identified in the EEVF (Fig. 1). Volcanic activity started ~0.46 Ma ago and migrated from the older nephelinitic, leucititic, and phonolitic centres in the northwest towards the basanitic to tephritic volcanoes (0.4–0.2 Ma) in the central and southeastern part of this field, and culminated in the cataclysmic eruption of the Laacher See volcano 13,000 years ago (Schmincke 2007 and references therein). Trace elemental and Sr–Nd–Pb–Os isotopic evidence suggested that basalts from the EEVF and of older Tertiary intraplate volcanism in Germany are of mixed asthenospheric origin with a contribution from hydrated amphibole/phlogopite-bearing metasomatised lithospheric mantle (Wörner et al. 1986; Bogaard and Wörner 2003; Jung et al. 2006, 2011). Positively correlated Nb/Ta and Lu/Hf along with low Zr/Nb and Zr/Sm observed in basalts from Eifel, Rhön, and Vogelsberg areas (Central Germany) have been attributed to carbonatite metasomatism within the subcontinental lithospheric mantle (Pfänder et al. 2012).

The Laacher See tephra

The phonolitic Laacher See volcano in the Quaternary EEVF (Fig. 1) erupted 13,000 years ago a volume of 6.3 km^3 of compositionally zoned phonolite magma (dense rock equivalent, Bogaard and Schmincke 1985; Baales et al. 2002). It has been divided into three main stratigraphic units, named LLST (Lower LST), MLST (Middle LST), and ULST (Upper LST) (Fig. 2). The deposit represents an inverted, chemically zoned phonolite magma column at 3–6 km depth, with mafic (ULST) and highly (LLST) differentiated phonolite representing the lowermost and uppermost erupted portion of the Laacher See magma

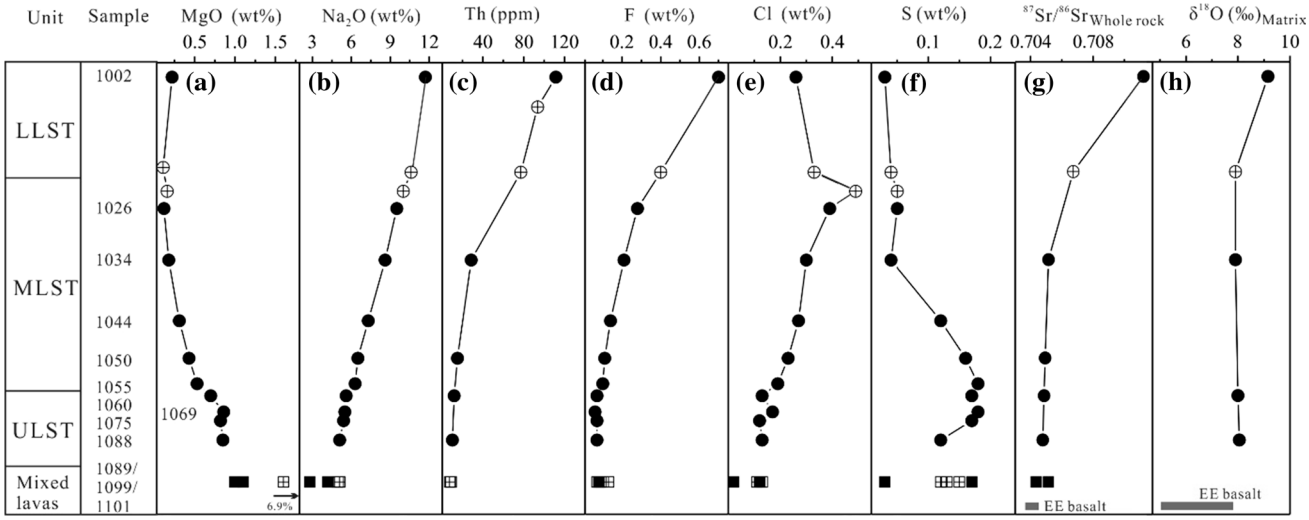

Fig. 2 Chemical and isotopic gradients within the Laacher See phonolite tephra, demonstrated by a few key elements and isotopes. Deposited tephra units (LLST, MLST, ULST) represent the inverted stratigraphic sequence in the magma chamber (i.e., magma chamber "stratigraphy"). For comparison, the Sr–O isotopic ranges for the East Eifel (EE) basalts are also shown. The $\delta^{18}O$ values of matrix in samples 1002 and 1088 were obtained based on sanidine $\delta^{18}O$ values and fractionation factors between sanidine and magma (Wörner et al. 1987). *Solid symbols* denote the samples investigated in this study, while *open symbols* with crosses denote the samples that were studied previously, but are not available for Cu isotopic measurements. The data are sourced from references (Wörner and Schmincke 1984a, Wörner et al. 1985, 1986, 1987)

chamber, respectively (Wörner and Schmincke 1984a, b). The structure, mineralogy, petrography, petrology, geochemistry, and petrogenesis of the LST have been discussed in detail elsewhere (Wörner et al. 1983, 1985, 1987; Wörner and Schmincke 1984a, b; Bogaard and Schmincke 1985).

Early erupted LLST pumice consists of nearly aphyric, highly differentiated phonolite with high total alkalis ($Na_2O + K_2O > 15$ wt%) and pre-eruptive volatiles (e.g., F and Cl up to 0.7 and 0.3 wt%, respectively). It is highly enriched in incompatible trace elements (e.g., Th) (Fig. 2b–e) and strongly depleted in Sr and other compatible elements (Wörner and Schmincke 1984a). The MLST represents the main volume of the LST and comprises moderately differentiated phonolite with increasing phenocryst contents (e.g., sanidine, plagioclase, amphibole, clinopyroxene, and sphene) as the eruption proceeded. The MLST phonolite chemically grades into the latest, phenocryst-rich, mafic phonolite (ULST) that represents the lowermost and last erupted part of the magma chamber. Final products are mingled basanite-phonolite hybrid magmas that contain mega-crystals (e.g., olivine, clinopyroxene) and rare peridotite nodules derived from the mafic basanite recharge magmas. Compositional gradients within the Laacher See magma chamber prior to eruption are overall continuous (Fig. 2), representing a magma series that formed mostly by fractional crystallization and magma mixing.

Based on major element data, a petrogenetic model for the evolution of the LST proposed by Wörner and Schmincke (1984a) and Wörner et al. (1985, 1987) suggests that the late-erupted mafic ULST phonolite originated from a parental basanite magma via 70 % fractional crystallization of clinopyroxene, amphibole, phlogopite, magnetite, olivine, and apatite (Stage I). A late study showed that during Stage I, FeS-saturation and sulfide fractionation occurred as revealed by the presence of numerous pyrrhotite globules within phenocrysts (e.g., clinopyroxene, amphibole) (Harms and Schmincke 2000). Higher $^{87}Sr/^{86}Sr$ ratios and $\delta^{18}O$ values in the mafic ULST phonolite than in its parental basanite (Fig. 2g, h) suggests slight contamination of a few percent of the magma system by radiogenic Sr and ^{18}O-enriched crustal materials (e.g., mica schist) during the Stage I (Wörner et al. 1985, 1987). Starting from the mafic ULST phonolite as a parent, the zoned sequence formed by progressive crystallization of the phenocryst phases (i.e., sanidine, plagioclase, hauyne, amphibole, clinopyroxene, sphene, apatite, Ti-magnetite, biotite, nepheline, cancrinite, and zircon) (Stage II) (Wörner and Schmincke 1984a, b). During Stage II, only minor assimilation of the Devonian sedimentary rocks (e.g., slate, greywacke) occurred (Wörner et al. 1985, 1987). Late-stage differentiation (Stage III) together with minor crustal contamination produced chemical and isotopic (e.g., O, Sr) disequilibrium between phenocrysts and matrix in the highly fractionated, volatile-rich cupola (Wörner et al. 1983, 1985, 1987). Cl/F relations with a reversal in the chlorine gradient (Fig. 2d, e) towards the top of the magma chamber, experimental data on H_2O solubility (Wörner and

Schmincke 1984a, b; Harms and Schmincke 2000; Berndt et al. 2001; Harms et al. 2004) as well as abundant carbonatite-syenites with degassing pipes and fenitisised country rocks from the carapace of the magma chamber indicate that its most evolved cupola was actively degassing an alkaline- and Cl-rich hydrous fluid prior to eruption. The extreme S depletion towards more evolved phonolite (Fig. 2f) also suggests that S might have been lost from the system through magma degassing (Wörner and Schmincke 1984a).

Wörner and Wright (1984) proposed that magma mixing occurred just prior to eruption (h/days) of the lowermost magma layer, as revealed by occurrence of a variety of the latest erupted hybrid rocks (mixed lavas) in the LST. The hybrid rocks formed by mixing between a crystal-rich phonolite from the base of the magma chamber and a newly recharged (megacryst-bearing) basanite magma (Wörner and Wright 1984).

Sample descriptions

Thirteen well-characterized samples covering the whole compositional and mineralogical spectrum of the LST, including one highly evolved LLST phonolite (1002) from the base of the sequence, five moderately differentiated MLST phonolites (1026, 1034, 1044, 1050, 1055), four mafic ULST phonolites (1060, 1069, 1075, 1088) and three hybrid rocks (1089, 1099, 1101) from the top of the deposit were analyzed for their Cu isotopic compositions. Phonolites have MgO from 0.12 to 0.86 wt% (Fig. 2a) and Cu from 1.12 to 3.95 ppm (Fig. 3a). Hybrid rocks range in MgO from 1.1 to 6.9 wt% (Fig. 2a) and Cu from 3.61 to 46.2 ppm (Fig. 3a).

Five basaltic lavas, three crustal xenoliths from the metamorphic basement (two granulites, one mica-schist), and two Devonian country rocks (slate, greywacke) from the East Eifel were also analyzed. Data for major and trace elements, as well as Sr–Nd–Pb–O–H isotopes have been published previously (Duda and Schmincke 1978; Wörner et al. 1982, 1986, 1987). Basaltic rocks include basanites, nephelinites, tephrites, and leucitites with MgO from 2.86 to 9.0 wt% (Duda and Schmincke 1978) and Cu from 31.9 to 61.5 ppm (Fig. 3a). Crustal rocks have Cu concentrations of 5.86 to 26.8 ppm (Fig. 3a). In addition, three basalts (one basanite and two nephelinites) from the West Eifel (WE) were also analyzed for their Cu isotopic compositions. These basalts have MgO from 2.93 to 3.25 wt% and Cu from 68.9 to 121.7 ppm (Fig. 3) (e.g., Mertes and Schmincke 1985).

Four mega-crystals (two clinopyroxene, one amphibole, and one phlogopite) from the LST were also analysed. These compositionally homogeneous mega-crystals represent high-pressure phases derived from parental

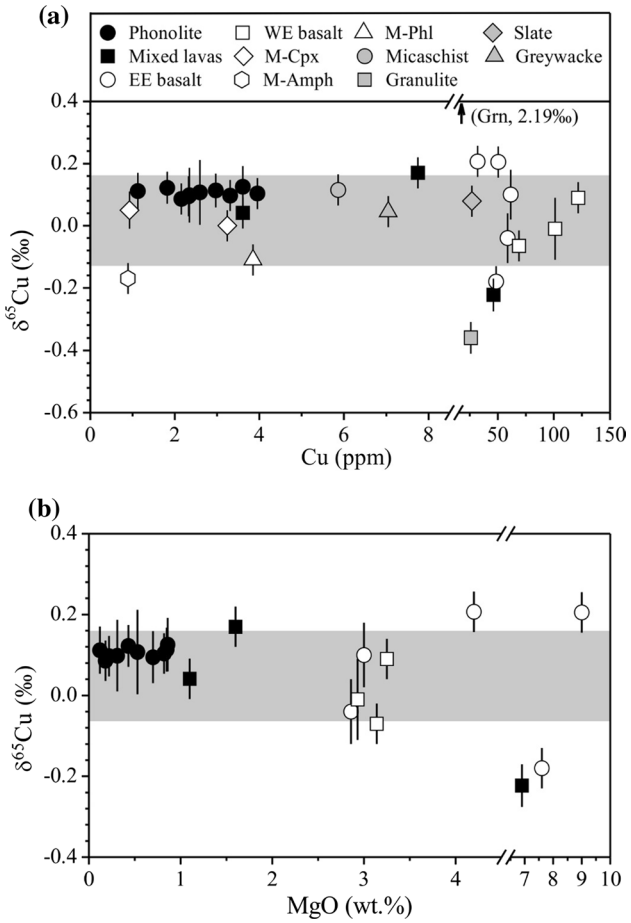

Fig. 3 δ^{65}Cu versus Cu in all studied samples (**a**) and δ^{65}Cu versus MgO in basalts and phonolites. For mega-amphibole (M-Amph) and mega-phlogopite (M-Phl), the average δ^{65}Cu values of two time repeated measurements and the long-term reproducibility (±0.05 ‰) are used. The *gray bar* denotes the available Cu isotopic range of MORB and OIB (δ^{65}Cu = −0.07 to 0.16 ‰, Liu et al. 2015a; Savage et al. 2015a). *EE* East Eifel, *WE* West Eifel, *M-Cpx* mega-clinopyroxene. Data are taken from Tables 2 and 3

basanite magmas (Wörner et al. 1985, 1987). Clinopyroxene 1099-2 is from a basanite-phonolite hybrid rock, has been analyzed for O and Sr isotope ratios previously (Wörner et al. 1985, 1987) and a powder was available for Cu isotope analysis. The other mega-crystals (up to ~3.0 × 2.0 × 0.6 cm^3) were crushed into small pieces, and clean mineral grains without visible inclusions and surficial alteration were handpicked under a binocular microscope. Several clean mineral grains were firstly mounted in epoxy resin and then polished down to expose grain centre. Laser-ICPMS analyses using the methods described by He et al. (2016) show that mega-crystals have Cu concentrations from 0.66 to 2.49 ppm (Fig. 3a). In addition to mounted mineral grains for LA-ICPMS analyses, the rest of handpicked mineral grains were used for Cu isotope analyses.

Analytical methods

Copper isotope ratios were measured using a sample-standard bracketing method on a *Neptune Plus* multi-collector inductively coupled plasma mass spectrometry (MC-ICP-MS) at the Isotope Geochemistry Laboratory of the China University of Geosciences, Beijing (CUGB). The detailed procedures for sample dissolution, column chemistry, and instrumental analysis can be found in Liu et al. (2014a, b, 2015a). Only a brief description is given below.

Sample dissolution and chemical purification

Handpicked mineral grains (i.e., amphibole, clinopyroxene, phlogopite) were firstly cleaned with mild double-distilled HF acid and then with MQ water before dissolution. The studied phonolites, hybrid rocks, and mega-crystals have low Cu concentrations from 1.12 to 7.75 ppm (Fig. 3a). In order to obtain at least 0.4 μg Cu for high-precision isotope analysis, ~50 to 360 mg samples were weighed. Once the required weight of one sample exceeds ~100 mg and depending on its Cu concentration, sub-samples were weighed into different Savillex screw-top beakers to dissolve and process them separately to prevent overload during the chemical purification process using ion-exchange chromatography. Whole rock and mineral samples were dissolved in a combination of double-distilled HF + HNO_3 + HCl. Copper was separated from the matrix elements in 8 N HCl + 0.001 % H_2O_2 using 2 mL pre-cleaned Bio-Rad AG-AP-1 M strong anion resin (100–200 mesh; chloride form). After the first column purification, the Cu-bearing fractions were evaporated to ~5 mL at 80 °C, and then 2–4 eluted Cu-bearing fractions of sub-samples divided from the same sample were merged into a single solution. The combined solutions were evaporated to dryness at 80 °C, and the residues were dissolved in 1 mL of 8 N HCl + 0.001 % H_2O_2 for a second main column purification step.

The main column procedure was firstly processed at least twice as did in previous studies (Liu et al. 2014a, b, 2015a), and matrix elements (i.e., Na, Fe, Ti) were checked for each eluted Cu solution. When high ratios of Na/Cu (>1), Fe/Cu (>0.5), and Ti/Cu (>0.2) occur, which can lead to a pronounced bias for Cu isotope analysis due to molecular spectral interference (Mason et al. 2004; Liu et al. 2014b), a further column chemistry was carried out. After the third run through column separation, the Cu yields were estimated to be ≥99.7 % based on analyses of Cu contents in the elution collected before and after the Cu cut. In addition, the ratios of (Na, Fe, Ti) to Cu were checked again and range from 0.04 to 0.89, ~0 to 0.04 and 0.09 to 0.17, respectively. Such low ratios yield negligible influence on the accuracy of Cu isotope analysis (Liu et al. 2014b). Finally, the eluted Cu solutions were evaporated to dryness, dissolved in 3 % (m/m) HNO_3, and then re-evaporated to dryness and re-dissolved in 3 % HNO_3 to remove all chlorine prior to isotope ratio analysis. The total procedural blank (from sample dissolution through repeated column chemistry to mass spectrometry) is 1.5 ng during the course of this study, which is considered negligible.

Instrumental analysis

Copper isotope analyses were carried out by a sample-standard bracketing method using a Thermo-Fisher *Neptune plus* MC-ICP-MS equipped with a PFA Teflon self-aspirating micro-nebulizer system. A SIS, a quartz dual cyclonic spray chamber, was used as the sample introduction system in this study. Copper isotope ratios were analyzed in low-resolution mode with ^{63}Cu in the Central cup and ^{65}Cu in the H2 Faraday cup. A measurement consists of three blocks of 40 cycles of ~8 s each during a first analysis step. In order to obtain high-quality data, nearly all purified stock solutions of unknown samples and standards were re-analyzed later. During the second analysis step, a measurement consists of two or three blocks. Thus each value reported is an average of 80 to 240 ratios. Cu isotope ratios are reported in standard δ-notation in per mil relative to standard reference material (SRM) NIST 976:

$$\delta^{65}Cu = \left(\left({}^{65}Cu/{}^{63}Cu \right)_{sample} / \left({}^{65}Cu/{}^{63}Cu \right)_{NIST\,976} - 1 \right) \times 1000$$

Precision and accuracy

During the course of this study, several international rock standards (e.g., BHVO-2, BIR-1a, BCR-2, and GSP-2) and an in-house Cu standard (GSB-Cu) were processed two or three times through column chemistry together with unknown samples and analyzed for Cu isotopic compositions. Repeated analyses yield the $\delta^{65}Cu$ values of 0.05 ± 0.04 ‰ (2SD, $n = 6$) for BIR-1a and 0.45 ± 0.05 ‰ (2SD, $n = 3$) for GSB-Cu (Table 1), suggesting that the long-term external reproducibility for $\delta^{65}Cu$ measurements is ±0.05 ‰ during the course of the data acquirement. In addition, the $\delta^{65}Cu$ values yielded in this study are 0.14 ± 0.05 ‰ (2SD) for BHVO-2, 0.17 ± 0.03 (2SD, $n = 2$) for BCR-2, and 0.32 ± 0.06 ‰ (2SD) for GSP-2 (Table 1). These data agree well within errors with those published in previous studies (e.g., Archer and Vance 2004; Mason et al. 2004; Li et al. 2009; Bigalke et al. 2010; Weinstein et al. 2011; Liu et al. 2014a, b, 2015a; Savage et al. 2015a). This, combined with the indistinguishable results from replicate analyses (Tables 2, 3), assures the accuracy of our data.

In order to further evaluate the accuracy of Cu isotope analyses on samples (e.g., phonolite) with low Cu

Table 1 Copper isotopic compositions of USGS reference materials, a synthetic solution, and pure Cu solutions

Standard[a]	Common	Column[b]	δ^{65}Cu[c]	2SD[d]	*N*[e]
BHVO-2	Basalt	3	0.14	0.05	3
BIR-1a	Basalt	2	0.05	0.04	5
		2	0.07	0.02	3
		2	0.04	0.00	2
		2	0.03	0.04	5
		2	0.05	0.05	5
		2	0.04	0.05	5
Average			**0.05**	**0.04**	**6**
BCR-2	Basalt	2	0.15	0.05	3
		2	0.19	0.08	3
Average			**0.17**	**0.03**	**2**
GSP-2	Granodiorite	3	0.32	0.06	4
Pure Cu	GSB solu1tion	2	0.46	0.02	5
		2	0.47	0.04	5
		2	0.42	0.03	5
Average			**0.45**	**0.05**	**3**
Phonolite–Cu	Synthetic solution	3	0.03	0.03	3

[a] Pure Cu solution contains only element Cu. Phonolite–Cu is a synthetic solution with concentration ratios of Al:K:Na:Fe:Ca:Ti:Mg:Mn:Cu = 42,600:27,500:27,000:8600:7000:1400:1200:640:1, which were chosen according to the average values of the investigated phonolites and one hybrid rock (1089) from the Laacher See tephra. If no Cu isotope fractionation occurred during column chemistry, δ^{65}Cu of the Phonolite–Cu solution should be close to zero

[b] The number of times column chemistry was processed in this study

[c] $\delta^{65}Cu = ((^{65}Cu/^{63}Cu)_{sample}/(^{65}Cu/^{63}Cu)_{NIST\ 976} - 1) \times 1000$, where NIST 976 is a Cu isotope standard and has a recommended value of $^{63}Cu/^{65}Cu = 2.2440 \pm 0.0021$ (Shield et al. 1965)

[d] 2SD = 2, two times the standard deviation of the population of n repeat measurements of a sample solution

[e] The number of repeated measurements of the same purification solution by MC-ICP-MS

contents and high ratios of cation (e.g., Na, Ti, Fe)/Cu, a synthetic multi-element solution (Phonolite–Cu) with concentration ratios of Ti:Al:Fe:Mn:Mg:Ca:Na:K:Cu = ~1410:42,640:8620:640:1190:6950:26,925:27,480:1 was made based on the average contents of these elements in the investigated phonolites and a hybrid rock (1089) from the LST. The Phonolite–Cu solution was divided into two aliquots that were separately processed through the first column purification step and then merged into a single solution using the method described above. The combined Phonolite–Cu solution was further purified two times. After the third column purification step, matrix elements of the purified Phonolite–Cu solution were checked. The ratios of (Na, Fe, Ti) to Cu are 0.07, 0.1, and 0.15, respectively. Analysis of the synthetic Phonolite–Cu yield a δ^{65}Cu value of 0.03 ± 0.03 ‰ (2SD) (Table 1), in agreement with the expected value of 0. This further suggests that the merging process and the three stage column chemistry induce negligible influence on Cu isotope analysis.

Results

Copper elemental and isotopic compositions of the studied rocks and mega-crystals are listed in Tables 2 and 3, respectively. All Cu isotopic data are plotted in Fig. 3a. Phonolites from the LST have homogeneous Cu isotopic compositions with δ^{65}Cu of 0.09–0.13 ‰, while hybrid rocks display variable δ^{65}Cu from −0.22 to 0.17 ‰. Basalts have δ^{65}Cu from −0.18 to 0.21 ‰, exceeding the range of global MORBs and OIBs (δ^{65}Cu = −0.07 to 0.16 ‰, Liu et al. 2015a; Savage et al. 2015a). Basement and country rocks have δ^{65}Cu from 0.05 to 0.12 ‰, while lower crustal granulite xenolith has highly variable δ^{65}Cu from −0.36 to 2.19 ‰. The δ^{65}Cu values of mineral mega-crystals range from −0.17 to 0.05 ‰. The δ^{65}Cu values of phonolites and basalts display no correlations with MgO contents (Fig. 3b).

Discussion

Chemical weathering and crustal contamination

Chemical weathering and crustal contamination have the potential to obliterate the original Cu isotopic composition of igneous rocks (e.g., Vance et al. 2008; Mathur et al. 2012; Liu et al. 2014a), and thus may hamper a straightforward interpretation of Cu isotopic data with respect to magma differentiation and degassing as well as the nature and composition of the melt source region. Thus, chemical weathering and crustal contamination require evaluating first. Several lines of evidence suggest that the effect of chemical weathering is limited on the elemental and isotopic compositions of the phonolites and basalts investigated here. First, petrological observations have shown that these rocks are free of secondary minerals (e.g., zeolite, iddingsite, or clay minerals) diagnostic of secondary alteration (Duda and Schmincke 1978; Wörner and Schmincke 1984a; Wörner et al.1985). Second, the LST phonolites show systematic variations and good correlations in major and trace element concentrations along the stratigraphy of the tephra deposit, which reflect the result of magma differentiation and degassing (Fig. 2a–f). This includes elements (e.g., Na, K, Rb, Sr) and element ratios (e.g., K/Ti) that would be highly sensitive to secondary alteration (Wörner and Schmincke 1984a, b). Third, partial hydration of pumice glasses by meteoric waters cannot be excluded; however, electron microprobe analyses of the glass do not indicate any disturbance of elements

Table 2 Copper isotopic compositions and selected elemental and isotopic ratios of the lavas and xenoliths from Eifel, Germany

Sample[a]	Unit[b]	Cl[c] wt%	S[c] wt%	MgO[c] wt%	$\delta^{18}O$[c] (‰)	$^{87}Sr/^{86}Sr$[c]	Cu[d] ppm	$\delta^{65}Cu$[e] ‰	2SD[f]	*N*[g]
Phonolites and hybrid rocks, Laacher See Volcano (13 ka)										
1002	LLST	0.26	0.03	0.22	9.15	0.71122	3.31	0.10	0.04	6
1026	MLST	0.39	0.05	0.12			1.12	0.11	0.06	6
1034	MLST	0.30	0.04	0.18	7.9	0.70514	2.15	0.09	0.03	6
1044	MLST	0.27	0.12	0.31			2.34	0.10	0.09	6
1050	MLST	0.23	0.16	0.43		0.70492	1.82	0.12	0.05	6
1055	MLST	0.19	0.18	0.53			2.59	0.11	0.10	6
1060	ULST	0.13	0.17	0.70	8.0	0.70486	2.32	0.09	0.06	6
1069	ULST	0.17	0.18	0.86			3.61	0.13	0.07	6
1075	ULST	0.12	0.17	0.82			3.95	0.10	0.02	6
1088	ULST	0.13	0.12	0.85	8.05	0.70477	2.97	0.11	0.05	6
1089	M.L	0.13	0.17	1.10			3.61	0.04	0.03	3
1099	M.L	0.11	0.17	1.60			7.75	0.17	0.04	5
1101	M.L	0.02	0.03	6.90		0.70513	46.2	−0.22	0.05	5
Replicate[h]								−0.20	0.03	4
Average								−0.21		
Mafic Quaternary alkaline lavas										
E41 Basanite				9.00	5.0	0.70470	50.4	0.21	0.04	5
E216 Basanite				7.60	5.7	0.70459	48.4	−0.18	0.05	3
E189 Tephrite				4.20	7.8	0.70464	31.9	0.21	0.05	5
LV3511 Leucitite				2.86		0.70462	58.8	−0.04	0.08	3
LV2803 Nephelinite				3.00		0.70442	61.5	0.10	0.08	3
M90 Basanite				3.14		0.70392	68.9	−0.07	0.01	2
ME9 Leuctite-nephelinite				2.93		0.70545	101.1	−0.01	0.10	3
NM359 Melilithe-nephelinite				3.25		0.70413	121.7	0.09	0.05	3
Xenoliths and local crustal rocks										
Micaschist (144)				1.31	11.7	0.74600	5.86	0.12	0.01	3
Slate (2004)				2.07	14	0.74500	26.8	0.08	0.03	3
Greywacke (2003)				1.04		0.72866	7.05	0.05	0.02	3
Granulite (398)				8.49		0.70472	19.8	2.19	0.01	3
Replicate								2.18	0.01	3
Granulite (395)				6.14	7.2	0.70515	26.0	−0.36	0.04	3

[a] Samples M90, ME9, and NM 359 are from West Eifel and others from East Eifel, both collected and previously analysed by Wörner et al. (1982), Wörner and Schmincke (1984a), and Wörner et al. (1985, 1986, 1987)

[b] The LLST, MLST, and ULST represent the lower, middle, and upper units of the Laacher See phonolitic tephra. M.L denotes mixed lavas (samples from Wörner and Schmincke 1984a)

[c] Element concentrations (i.e., MgO, F, Cl, and S) and O–Sr isotopic compositions are taken from the references (Wörner and Schmincke 1984a; Wörner et al. 1985, 1986, 1987). Matrix $\delta^{18}O$ values and whole $^{87}Sr/^{86}Sr$ ratios are used here. The matrix $\delta^{18}O$ value of sample 1002 was calculated from that of sanidine

[d] Copper concentrations measured by comparison of signal intensities with 100 ppb GSB Cu, an in-house standard (Liu et al. 2014b)

[e] $\delta^{65}Cu = ((^{65}Cu/^{63}Cu)_{sample}/(^{65}Cu/^{63}Cu)_{NIST\ 976} - 1) \times 1000$, where NIST 976 is an international Cu isotope standard

[f] 2SD = 2, two times the standard deviation of the population of n repeat measurements of a sample solution

[g] *N* represents the times of repeat measurements of the same purification solution by MC-ICP-MS

[h] Replicate denotes the repeated sample dissolution, column chemistry, and mass spectrometry

(e.g., alkalies) that are sensitive to secondary alteration (Wörner and Schmincke 1984a; Bogaard and Schmincke 1985).

Copper isotope analyses show that slate, greywacke, and mica-schist have the normal mantle-like Cu isotopic compositions, while two granulites show a large $\delta^{65}Cu$ range

Table 3 Copper isotopic compositions of megacrysts from phonolites in the Laacher See tephra

Sample[a]	δD (‰)[b]	Cu (ppm)[b]	$\delta^{65}Cu$[c]	2SD[d]	*N*[e]
1099-2Cpx		3.24	0.00	0.03	3
1083Cpx		0.77 ± 0.71 ($n = 9$)	0.05	0.06	3
LSTM Amph	−27	0.66 ± 0.90 ($n = 6$)	−0.15	0.05	3
Replicate[f]			−0.19	0.03	3
Average			−0.17		
1083Phl	−38	2.49 ± 4.59 ($n = 10$)	−0.09	0.03	3
Replicate			−0.13	0.01	3
Average			−0.11		

[a] Cpx = Clinopyroxene, Amph = Amphibole, Phl = Phlogopite

[b] Copper concentrations for 1099-2Cpx measured by comparison of signal intensities with 100 ppb GSB Cu, an in-house standard (Liu et al. 2014b). Average Cu concentrations of other mineral separates were obtained by multiple analyses of different grains of the same mineral using LA-ICPMS at the University of Science and Technology of China (USTC). Detailed analytical procedures can be found in He et al. (2016). The numbers after ± represent two standard deviations of the results from multiple analyses (*n*)

[c] $\delta^{65}Cu = ((^{65}Cu/^{63}Cu)_{sample}/(^{65}Cu/^{63}Cu)_{NIST\ 976} - 1) \times 1000$, where NIST 976 is an international Cu isotope standard

[d] 2SD = 2, two times the standard deviation of the population of n repeat measurements of a sample solution

[e] *N* represents the number of repeat measurements of the same purification solution by MC-ICP-MS

[f] Replicate denotes the repeated sample dissolution, column chemistry, and mass spectrometry. Repeated analyses were carried out on *Neptune Plus* MC-ICPMS at the Metal Stable Isotope Laboratory in the USTC

from −0.36 to 2.19 ‰, encompassing the Cu isotopic range of the mega-crystals and Quaternary basalts from Eifel (Fig. 3a). This indicates that assimilation of lower crustal granulite could modify Cu isotopic compositions of the basaltic magmas. However, comprehensive studies have demonstrated that the genesis of the Quaternary Eifel basalts involved insignificant crustal contamination/assimilation given their OIB-like distribution patterns of trace elements, occurrence of mantle xenoliths, and the absence of correlation between the differentiation index (e.g., Mg#) and radiogenic isotopic compositions (e.g., $^{87}Sr/^{86}Sr$) (e.g., Wörner et al. 1986; Pfänder et al. 2012).

The geochemical evolution of the Laacher See zoned magma chamber can be divided into three main stages (Wörner and Schmincke 1984a; Wörner et al. 1985). Stage I, generation of mafic phonolite through differentiation of a parental basanite magma via crystal-melt fractionation; Stage II, formation of the zoned phonolite column by closed-system progressive crystal-melt fractionation within a crustal magma chamber; and Stage III, a late-stage differentiation that produced some of the unusual trace element variations in certain samples (e.g., sample 1002). More radiogenic $^{87}Sr/^{86}Sr$ in the ULST mafic phonolites than in the parental basanites (Fig. 2g) indicates limited assimilation of a crustal component during the Stage I. However, a quantitative calculation suggests only approximately 1–2 % assimilation of basement rocks (i.e., mica-schist) into a differentiating parental basanite magma (Wörner et al. 1985). One mica-schist analyzed here has $\delta^{65}Cu$ of 0.12 ‰ comparable to the East Eifel basanites (−0.18 to 0.21 ‰, Fig. 3a), but has a much lower Cu concentration (5.9 vs ~50 ppm, Tables 2, 3). Thus, 1–2 % assimilation of mica-schist have limited effect (~2 %) on the Cu concentration and thus would not change the Cu isotopic composition of the magma during differentiation.

Wörner et al. (1985) showed that a very small crustal component (i.e., greywacke, slate) was involved during Stage II. This precludes any significant effects on the major and trace element concentrations of the phonolite magma, and thus on their Cu isotopic compositions. During Stage III, assimilation of 0.2 % Devonian composite (slate/greywacke = 2/1) is allowed by radiogenic isotope data (Wörner et al. 1985). The slate and greywacke have Cu concentrations and $\delta^{65}Cu$ values of 26.8 ppm and 0.08 ± 0.03 ‰, and 7.05 ppm and 0.05 ± 0.02 ‰, respectively (Table 2). Thus, the Devonian composite has a Cu concentration of 20.2 ppm and a $\delta^{65}Cu$ value of 0.075 ‰, respectively. 0.2 ‰ assimilation of such composite into the most differentiated phonolite (represented by the LLST sample 1002 with a Cu concentration of 3.31 ppm, Table 2) elevates its Cu concentrations by only ~1.2 %. Considering all possible assimilants, including upper crustal Devonian composite (e.g., slate and greywacke), metamorphic basement (i.e., mica-schist), and lower crustal granulite, bulk assimilation models clearly exclude a significant influence of crustal contamination/assimilation on the Eifel basalts and the evolved phonolites (Wörner et al. 1986). This limited assimilation resulted in insignificant changes in their Cu isotopic compositions.

Phonolite and basalt Cu isotopic characteristics

We here firstly evaluate the behavior of Cu isotopes during fractional crystallization and degassing during phonolite magma differentiation and then discuss the cause for the heterogeneous Cu isotopic compositions of the Eifel basalts.

Phonolite magma differentiation and degassing

The LST phonolites are highly differentiated and experienced extensive magma degassing from the most evolved gas-rich cupola of the zoned magma chamber (Wörner and Schmincke 1984a, b). Thus, Cu isotope measurements of the chemically diverse phonolite enable us to evaluate Cu

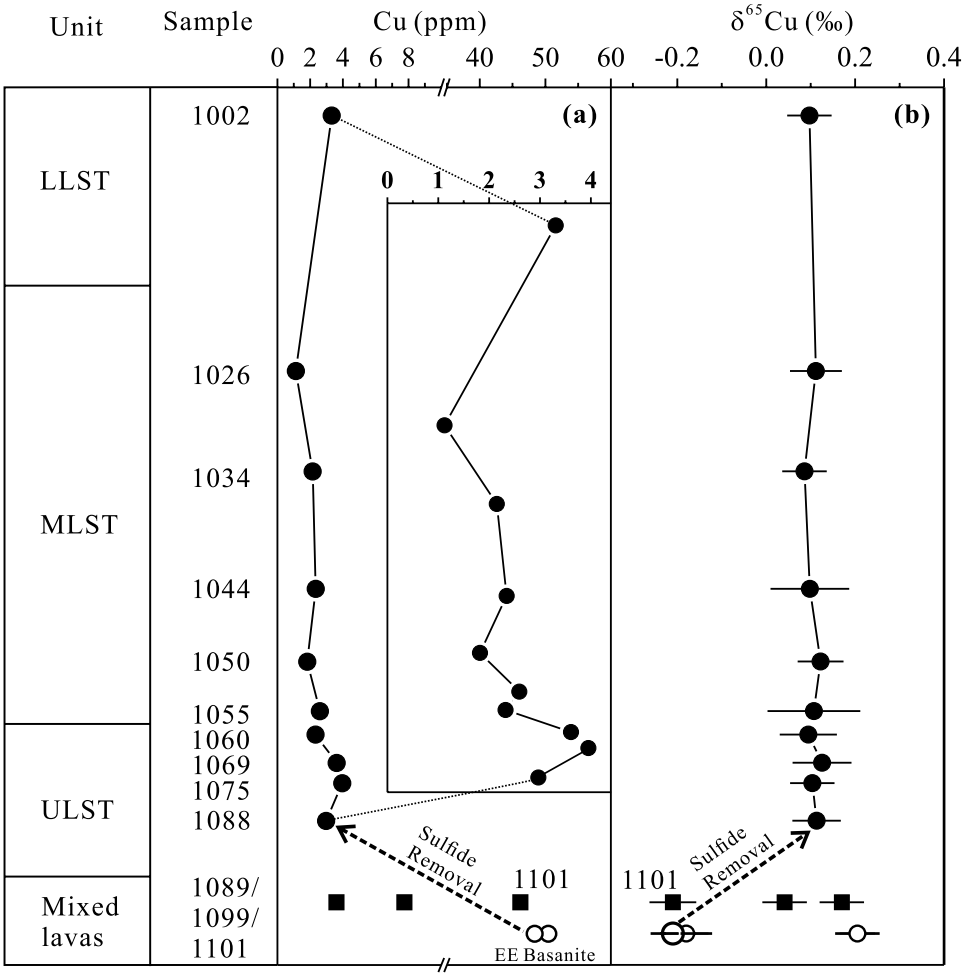

Fig. 4 Spatial variations of Cu elemental (**a**) and isotopic (**b**) compositions of the LST phonolites, hybrid rocks and EE basanites. For clarity, the *insert* in (**a**) only displays Cu concentrations in the LST phonolites. The largest *open circle* in (**b**) denotes the Cu isotopic composition of the hypothetical parental basanite magmas of the mafic ULST phonolites. This value (−0.21 ‰) was obtained by mass balance calculations based on the most Cu-rich hybrid rock 1101 (see details in text). *Dashed lines* with *arrows* represent the evolution paths of Cu elemental and isotopic compositions caused by sulfide fractionation during the differentiation from the parental basanite magmas to the mafic ULST phonolites. Data are taken from Table 2

isotope behavior during extreme magma differentiation and degassing. Major element data show that the late-erupted, mafic ULST phonolite originated from a parental basanite by fractional crystallization of clinopyroxene and amphibole with small amounts of phlogopite, magnetite, olivine, and apatite (Wörner and Schmincke 1984b). All these minerals have $D_{Cu}^{mineral–melt}$ of <1 (e.g., Gaetani and Grove 1997; Fellows and Canil 2012; Liu et al. 2014c, 2015b), suggesting that their fractional crystallization cannot explain much lower Cu concentrations of the mafic ULST phonolite (<4 ppm) compared to those of the parental basanite (~50 ppm) (Fig. 4a). Thus, fractional crystallization of sulfide with high $D_{Cu}^{sulfide/melt}$ (250–960, Gaetani and Grove 1997) must have occurred during the differentiation from the parental basanite magma to the mafic ULST phonolite (Stage I), and this is the most reasonable explanation for the strong Cu depletion in the latter. Sulfide fractionation is also consistent with a FeS saturation state and a relatively low oxygen fugacity in the mafic phonolitic magmas, evidenced by the occurrence of numerous pyrrhotite globules within phenocrysts (e.g., clinopyroxene, amphibole) and low S^{6+}/S_{total} ratio (as low as 0.08) in the mafic ULST phonolites (Harms and Schmincke 2000).

It is necessary to constrain the Cu isotopic composition of the parental basanite magma before evaluating the Cu isotope behavior during Stage I. The measured hybrid rocks have been petrologically and geochemically demonstrated to be formed by mixing of an evolved phonolite containing variable amounts of phenocrysts and a megacrystal-bearing basanite magma (Wörner and Wright 1984) and thus can be used to resolve this issue. The hypothetical megacrystal-bearing basanite magma can be regarded as the direct parental magma of the mafic ULST phonolite. The most Cu-rich hybrid rock (i.e., sample 1101) has a Cu concentration of 46.4 ppm, which is very similar to the basanites (~50 ppm) (Fig. 4a), suggesting that it must have a Cu isotopic composition close to that of the parental magma. Assuming that the parental basanite magma has a Cu content of 50 ppm and that the Cu elemental and isotopic compositions of the evolved phonolite endmember are denoted by those of the LST phonolites (average [Cu] = 2.57 ppm and $\delta^{65}Cu$ = 0.11 ‰), mass balance calculation based on

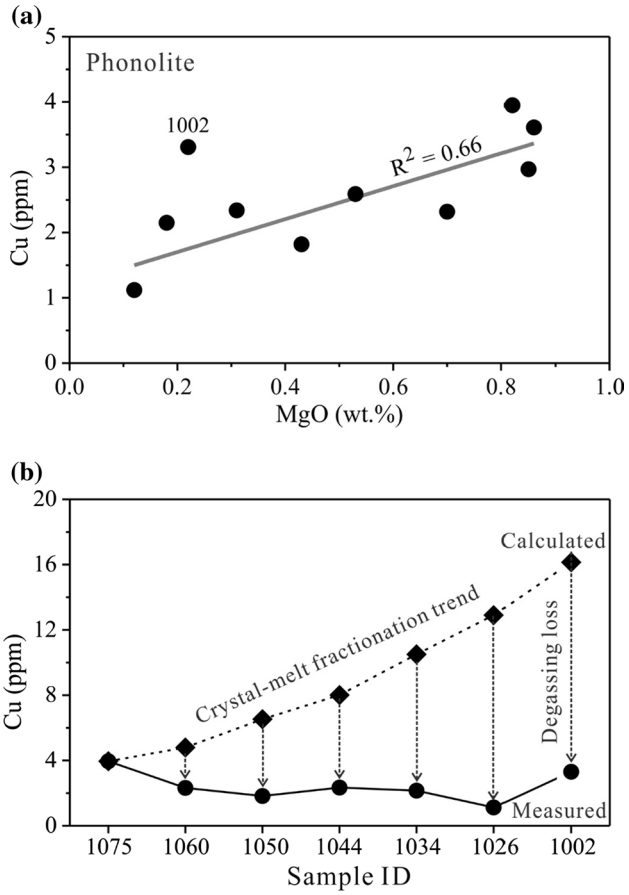

Fig. 5 Cu versus MgO (**a**) and comparison of modelled and measured Cu contents (**b**) in the LST phonolites. The *gray line* in (**a**) denotes a regression line using phonolite samples except 1002. The method for crystal-melt fractionation calculations was described in detail elsewhere (Wörner and Schmincke 1984b). In this calculation, the evolution path is from 1075 through 1060, 1050, 1044, 1034, and 1026 to 1022. The starting material is set as the mafic ULST phonolite 1075, and the derivative derived from the last step calculation is taken as the parental magma of the next step derivative (e.g., 1075 is the parent of 1060, while 1060 is the parent of 1050). The mineral phases fractionated and their relative modal abundance at each step used in our calculation were taken from Table 2 in this study of Wörner and Schmincke (1984b). The experimentally determined $D_{Cu}^{minerals/dacitic\ melts}$ were used and taken from Liu et al. (2014c, 2015b). The D_{Cu} is 0.115 for plagioclase (Run D8), 0.465 for magnetite (average of Run 3, 9, 14), 0.103 for amphibole (average of Run D9-11), 0.299 for clinopyroxene (average of Run D2-8, 14) and 0.091 for olivine (average of Run Cu-5, 30, 31, 46, 50, 55). No D_{Cu} for apatite is available in literatures, and the measured D_{Cu} for hauyne using mineral-whole rock pairs in the LST phonolites ranges from 1.0 to 9.9, with an average of 3.3 (Feige 2011). We found that the selection of D_{Cu} (e.g., 0–10) for hanyue and apatite has very limited effects on the calculated Cu contents because of their low modal abundance in the fractionated assemblages. Thus, the D_{Cu} for apatite is arbitrarily set as 0.115, equivalent to that of plagioclase, and for hauyne the average value of 3.3 was used in our calculation. The Rayleigh fractionation model was used: $C_L = C_0 f^{(D-1)}$, where C_0 and C_L denotes the Cu contents in the parental and residual (derivative) magmas, respectively; f is the mass fraction of residual magma (i.e., derivative fraction, see Table 2 in Wörner and Schmincke (1984b)); $D = \sum D_i X_i$, where D_i and X_i are Cu partition coefficients and modal abundances for each mineral phases crystallized. It is noted that the calculated Cu contents in the derivative melts formed by fractional crystallization are much higher than those measured in the phonolites, suggesting that Cu was lost through volcanic degassing during the differentiation from mafic to highly evolved phonolites

the hybrid rock 1101 suggests that the parental basanite magma has a δ^{65}Cu value of −0.21 ‰. This value is lighter than that of the mafic ULST phonolite (Fig. 4b), suggesting that sulfide fractionation has preferentially removed the lighter Cu isotope (^{63}Cu) from the mafic parental basanite magmas. This is consistent with the experimental results that sulfide is enriched in the lighter Cu isotope (^{63}Cu) relative to the co-existing silicate, although large uncertainties exist (Savage et al. 2015a). Our result is also in accordance with the observation that in the S-saturated system, sulfide fractionation could cause resolvable Cu isotope fractionation (Savage et al. 2015b).

Progressive crystallization of a variety of minerals, including mostly sanidine, plagioclase, hauyne, amphibole, clinopyroxene, sphene, apatite, Ti-magnetite, and biotite, leads to the formation of the zoned phonolite column starting from the mafic ULST phonolite (Stage II) (Wörner and Schmincke 1984a, b). Systematic variations in major and trace element concentrations of phonolites in the LST (Fig. 2a-f) document this magma differentiation process. Except for hauyne with D_{Cu} ranging from 1.0 to 9.9 (Feige 2011), experimentally determined partitioning coefficients have demonstrated that Cu is incompatible in the above minerals crystallized during Stage II (e.g., Gaetani and Grove 1997; Fellows and Canil 2012; Liu et al. 2014c, 2015b), suggesting that Cu contents should increase with magma differentiation or the decrease of MgO contents in magmas. However, except for sample 1002, the phonolites display a positive correlation between Cu and MgO contents (Fig. 5a), suggesting that Cu was lost during fractional crystallization. The modelling calculation (see the detailed procedure in the caption of Fig. 5b), using the method described by Wörner and Schmincke (1984b), however, shows that the calculated Cu contents in the derivative melts formed by fractional crystallization during Stage II are much higher than those of the studied phonolites (Fig. 5b). These observations suggest that in addition to the above-mentioned minerals, certain minerals (e.g., sulfide) in which Cu is compatible might have been removed from the phonolitic magmas and/or that another process (e.g., degassing) had worked on the LST phonolites and lowered their Cu contents. Sulfur is depleted towards the LLST (Fig. 2f), while Cu shows only a minor decrease (except for most evolved sample 1002) (Fig. 4a). This suggests that some S may be fractionated by hauyne that contains up to 7 wt% S (Feige 2011) and additionally

may be lost due to degassing. However, Cu and its isotopes are unlikely to be controlled by sulfide fractionation during Stage II. That is, the melts were sulfide-undersaturated and thus removal of sulfide can be ruled out during the evolution from mafic to highly differentiated phonolites. This is consistent with the lack of pyrrhotite and high S^{6+}/S_{total} ratio (as high as 0.71) in the highly differentiated phonolites, which suggest a relatively high oxygen fugacity in the highly evolved phonolitic magmas (Harms and Schmincke 2000).

Previous studies have demonstrated that Cu can be significantly lost via magma degassing (e.g., Halter et al. 2005). Degassing upon cooling of MLST and LLST magmas prior to or at eruption is the preferred mechanism causing the observed decreasing S concentrations (Figs. 2f) (Wörner and Schmincke 1984a). Higher Cl concentrations in phonolites from the uppermost MLST compared to those from the lower LLST (Fig. 2e) indicate that Cl might have been released by leakage of a Cl-rich vapour phase from the early erupted most evolved magma layer (LLST) (Wörner and Schmincke 1984a). Active degassing from the cupola of the magma chamber is also indicated by many syenites that originate as cognate lithice from the cooler outer portions of the phonolite magma chamber. These rocks represent a crystallized carapace and have abundant degassing pipes with vapor phase deposits. In addition, country rocks are abundant and impregnated (fenitised) by alkali-rich fluids as documented by sanidine-aegirine veins. These geochemical and petrological evidence clearly demonstrate that the LST phonolites experienced extensive magma degassing associated with significant volatile losses (e.g., F, Cl, S; Wörner and Schmincke 1984a; Harms and Schmincke 2000). Copper partition experiments between vapor and melt have shown that Cu can be transported in a significant quantity by chloride and sulfide complexes (e.g., $CuCl(H_2O)$, Cu_3Cl_3 and $Cu(HS)(H_2S)^0$) in magmatic vapor (e.g., Simon et al. 2006; Etschmann et al. 2010). Thus, significant loss of Cu in the form of chloride and sulfide complexes during magma degassing is the most reasonable explanation for the offset between the modelled and measured Cu contents (Fig. 5b).

In terms of Cu isotopic data, the lack of correlation between $\delta^{65}Cu$ and MgO in the phonolite (Fig. 3b) suggests that no measurable Cu isotope fractionation occurred during the evolution of phonolite magmas toward their extreme fractionation product (sample 1002). This is consistent with the previous observation that Cu isotope fractionation is limited during crystal-melt fractionation in the sulfide-undersaturated system (Savage et al. 2015b). Quantum chemical calculations have shown that vapor-phase Cu complexes (e.g., $CuCl(H_2O)$, Cu_3Cl_3) display an enrichment of ^{65}Cu relative to liquid-phase Cu complexes (e.g., $Cu(HS)_2^-$, $CuCl_2^-$) with $\Delta^{65}Cu_{vapor-liquid}$ of up to 0.45 ‰ at 600 °C (Seo et al. 2007; Fujii et al. 2013, 2014), suggesting that ^{63}Cu becomes depleted in the vapor. However, Rempel et al. (2012) observed a shift in the opposite direction and obtained an experimentally determined $\Delta^{65}Cu_{vapor-liquid}$ of −0.10 ‰ at 450 °C, suggesting that ^{63}Cu becomes enriched in the vapor. Our results, based on studies of natural highly differentiated igneous rocks, show that $\delta^{65}Cu$ values of the LST phonolites are uniform and display no correlation with volatile contents (i.e., Cl, S) (Fig. 6). The potential implications of these findings are (1) that volcanic degassing during phonolite magma differentiation did not cause detectable Cu isotope fractionation, or more likely (2) that Cu isotope fractionation has occurred during volcanic degassing, but did not alter the bulk Cu isotopic compositions of the magma due to mass balance constraints. The latter case has been observed for Zn isotopes in andesitic rocks at Merapi volcano (Toutain et al. 2008).

Hybrid rocks that formed by mixing of highly evolved phonolite magma with the parental basanite (Wörner and Wright 1984) have variable Cu isotopic compositions lying between those of phonolites and basanites (Figs. 3a), which would be expected after magma mixing.

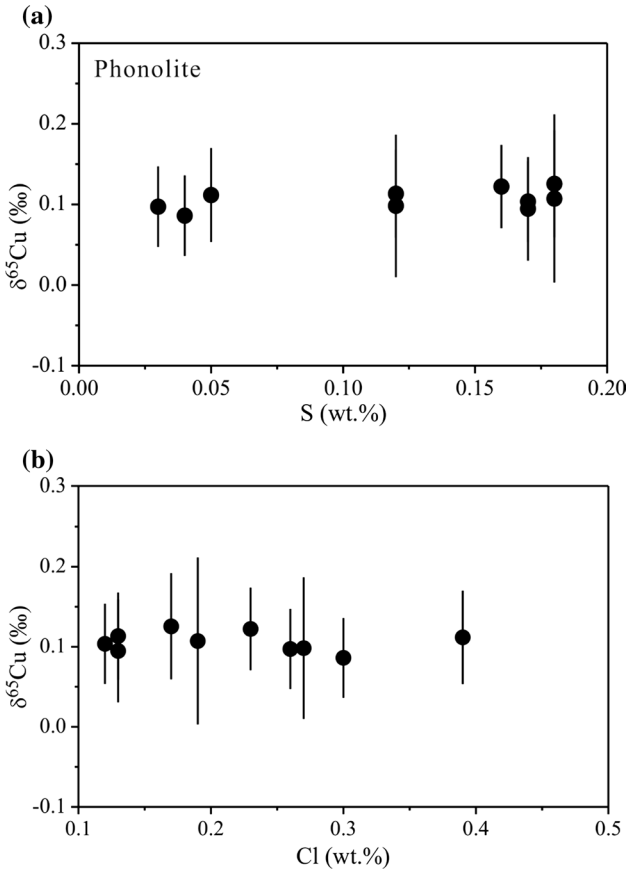

Fig. 6 $\delta^{65}Cu$ versus S (**a**) and Cl (**b**) in the LST phonolites. Data are taken from Table 2

Heterogeneous Cu isotopic compositions in Eifel basalts

The Eifel basalts and mega-crystals have δ^{65}Cu values of −0.18 to 0.21 ‰, exceeding the range defined by MORBs and OIBs (Fig. 3a, −0.07 to 0.16 ‰; Liu et al. 2015a; Savage et al. 2015a). Such Cu isotopic variations cannot be explained by isotope fractionation during basalt magma differentiation, as discussed below. High partition coefficients between sulfide and melts ($D_{Cu}^{sulfide/melt}$ ~ 250 to 960, Gaetani and Grove 1997) indicate that sulfide saturation is a key cause for the sudden drop in Cu contents of lavas (Jenner et al. 2010; Lee et al. 2012). Low $D_{Cu}^{silicate\ mineral/melt}$ (<1, e.g., Gaetani and Grove 1997; Fellows and Canil 2012; Liu et al. 2014c, 2015b) suggests that Cu contents in basaltic lavas should increase with crystallization of silicate minerals in the residual melts (decreasing MgO contents) under conditions of sulfide undersaturation. In addition, sulfide fractionation preferentially removes the lighter Cu isotope (^{63}Cu) and shifts the residual magmas to heavier Cu isotopic compositions (Savage et al. 2015a; this study). The absence of a sharp drop and in fact of any correlation in Cu contents with variable MgO contents in the basalts (Table 2) and the lack of correlations between δ^{65}Cu with Cu (Fig. 3a) imply that sulfide fractionation is not the cause for variable Cu isotope compositions of the Eifel basalts. Two lines of evidence suggest that silicate mineral crystallization also did not affect significantly Cu isotopes during the Eifel basalt differentiation. First, δ^{65}Cu values of these basalts show no correlation with MgO contents (Fig. 3b). Second, tephrite evolved from basanite magmas by crystallization of clinopyroxene, olivine, amphibole, and phlogopite (Duda and Schmincke 1978; Wörner and Schmincke 1984b) has similar Cu isotopic compositions to basanites (Table 2). Thus, the Cu isotopic compositions of the Eifel basalts must reflect the characteristics of the sub-Eifel mantle, which is consistent with earlier conclusions about isotopic heterogeneity in the mantle source of these Eifel basalts (Wörner et al. 1986).

Significant Cu isotopic variations (−0.19 to 0.47 ‰) of continental basalts from the North China Craton and arc lavas from Kamchatka have been observed by Liu et al. (2015a). They attributed such Cu isotopic variations to the involvement of recycled crustal materials in their mantle source regions. Mantle metasomatism was also proposed to explain the highly variable Cu isotopic compositions (−0.64 to 1.10 ‰) observed in metasomatized peridotite xenoliths (Savage et al. 2014; Liu et al. 2015a). Geochemical and isotopic (e.g., Sr–Nd–Pb) studies show that the petrogenesis of the Eifel basalts, like other intra-plate basalts in central Europe, involved the hydrated amphibole/phlogopite-bearing metasomatized lithospheric mantle (e.g., Wörner et al. 1986; Bogaard and Wörner 2003; Jung et al. 2006, 2011; Pfänder et al. 2012). Such hydrous mineral-bearing lithospheric mantle records one Hercynian metasomatic event as revealed by trace elemental and Sr–O–H isotopic studies of mantle xenoliths from Eifel (Witt-Eickschen and Kramm 1998; Kempton et al. 1988; Witt-Eichschen et al. 2003). These studies have shown that this metasomatic event is characterized by the presence of phlogopite- and/or amphibole-bearing peridotite xenoliths, LREE enrichments and relatively high ^{87}Sr/^{86}Sr (0.7041) of clinopyroxenes, ^{18}O-enrichments ($\delta^{18}O_{SMOW}$ up to 6.3 ‰) of olivines, and D-enrichments (δD_{SMOW} up to −45 ‰) of phlogopite and amphibole. These features have been attributed to mantle metasomatism by fluids derived from the subducted hydrothermally altered oceanic lithosphere. Heavier δD (−38 to −27 ‰) of mega-crystals investigated here (Table 2) relative to that of the mantle (−80 ‰) has been interpreted as the result of the addition of D-rich fluids derived from recycled seawater-altered oceanic crust into the sub-Eifel mantle (Wörner et al. 1987). Based on these observations, we proposed that mantle metasomatism by slab-derived fluids might have resulted in the heterogeneous Cu isotopic compositions of the Eifel basalts and mega-crystals.

Conclusions

High-precision Cu isotopic measurements on a cogenetic series of moderately to highly differentiated phonolites, their parental basalts, mega-crystals (i.e., clinopyroxene, amphibole, phlogopite), and crustal rocks (i.e., granulite, micaschist, slate, greywacke) from Eifel, Germany lead to the following conclusions:

1. The sudden drop of Cu contents during the evolution of the parental basanite magmas to the mafic ULST phonolites is indicative of sulfide fractionation. The heavier Cu isotopic compositions of the latter (~0.11 ‰) relative to those of the former (~−0.21 ‰) suggest that sulfide fractionation preferentially removes the lighter Cu isotope (^{63}Cu) in the S-saturated system.
2. The limited Cu contents (1.12–3.95 ppm) and no systematic variations of Cu with S suggests that sulfide removal must not occur during magma differentiation from mafic to highly evolved phonolites. The homogeneous Cu isotopic compositions ($\delta^{65}Cu = 0.11 \pm 0.03$ ‰, 2SD, $n = 10$) of the chemically diverse, cogenetic phonolites suggest a lack of any detectable Cu isotope fractionation by fractional crystallization of silicate, oxide and phosphate during phonolite magma differentiation.
3. No correlations between Cu isotopic compositions and volatile contents (e.g., S, Cl) are observed in the LST phonolites. This potentially implies that volcanic

degassing causes no detectable Cu isotope fractionation or that fractionation of Cu isotopes during volcanic degassing did not alter the Cu isotopic compositions of the LST phonolites.

4. The Eifel basalts and mega-crystals have variable δ^{65}Cu values of −0.18 to 0.21 ‰, which display no correlation with MgO, suggesting that such Cu isotopic variations were not caused by magma differentiation and must reflect the heterogeneity of the sub-Eifel mantle. Mantle metasomatism by fluids derived from the subducted oceanic lithosphere is most likely the mechanism for causing this Cu isotopic heterogeneity.

Acknowledgment J.H. thank D.D. Li and Y.W. Lv for help in the clean lab. This work is financially supported by Grants from the National Natural Science Foundation of China (NOs. 41573018, 41303015) to J.H and (NO. 4147301) to S.A.L. Thanks are due to Dr. Ryan Mathur and two anonymous reviewers for their constructive and thorough comments, which greatly improve this contribution. We also thank Dr. Jochen Hoefs for his efficient editorial handling work.

References

Albarède F (2004) The stable isotope geochemistry of copper and zinc. Rev Mineral Geochem 55:409–427

Archer C, Vance D (2004) Mass discrimination correction in multiple-collector plasma source mass spectrometry: an example using Cu and Zn isotopes. J Anal At Spectrom 19:656–665

Baales M, Jöris O, Street M, Bittmann F, Weniger B, Wiethold J (2002) Impact of the Late Glacial eruption of the Laacher See volcano, central Rhineland, Germany. Quat Res 58:273–288

Balistrieri LS, Borrok DM, Wanty RB, Ridley WI (2008) Fractionation of Cu and Zn isotopes during adsorption onto amorphous Fe(III) oxyhydroxide: experimental mixing of acid rock drainage and ambient river water. Geochim Cosmochim Acta 72:311–328

Berndt J, Holtz F, Koepke J (2001) Experimental constraints on storage conditions in the chemically zoned phonolitic magma chamber of the Laacher See volcano. Contrib Miner Petrol 140:469–486

Bigalke M, Weyer S, Wilcke W (2010) Copper isotope fractionation during complexation with insolubilized humic acid. Environ Sci Technol 44:5496–5502

Bogaard Pvd, Schmincke H-U (1985) Laacher See tephra: a widespread isochronous late Quaternary tephra layer in central and northern Europe. Geol Soc Am Bull 96:1554–1571

Bogaard PJF, Wörner G (2003) Petrogenesis of basanitic to tholeiitic volcanic rocks from the Miocene Vogelsberg, Central Germany. J Petrol 44:569–602

Duda A, Schmincke HU (1978) Quaternary basanites, melilite nephelinites and tephrites from the Laacher See area (Germany). Neues Jahrbuch fuer Mineralogie Abhandlungen 132:1–33

Etschmann BE, Liu W, Testemale D, Müller H, Rae NA, Proux O, Hazemann JL, Brugger J (2010) An in situ XAS study of copper(I) transport as hydrosulfide complexes in hydrothermal solutions (25–592 °C, 180–600 bar): speciation and solubility in vapor and liquid phases. Geochim Cosmochim Acta 74:4723–4739

Ehrlich S, Butler I, Halicz L, Rickard D, Oldroyd A, Matthews A (2004) Experimental study of the copper isotope fractionation between aqueous Cu(II) and covellite, CuS. Chem Geol 209:259–269

Feige J (2011) Verteilung und Fraktionierung der Spurenelemente in Mineralen des Laacher See Phonoliths: Eine LA ICP-MS Studie. Master's Thesis

Fellows SA, Canil D (2012) Experimental study of the partitioning of Cu during partial melting of Earth's mantle. Earth Planet Sci Lett 337–338:133–143

Fernandez A, Borrok DM (2009) Fractionation of Cu, Fe, and Zn isotopes during the oxidative weathering of sulfide-rich rocks. Chem Geol 264:1–12

Fujii T, Moynier F, Abe M, Nemoto K, Albarede F (2013) Copper isotope fractionation between aqueous compounds relevant to low temperature geochemistry and biology. Geochim Cosmochim Acta 110:29–44

Fujii T, Moynier F, Blichert-Toft J, Albarède F (2014) Density functional theory estimation of isotope fractionation of Fe, Ni, Cu, and Zn among species relevant to geochemical and biological environments. Geochim Cosmochim Acta 140:553–576

Gaetani GA, Grove TL (1997) Partitioning of moderately siderophile elements among olivine, silicate melt, and sulfide melt: constraints on core formation in the Earth and Mars. Geochim Cosmochim Acta 61:1829–1846

Halter W, Heinrich C, Pettke T (2005) Magma evolution and the formation of porphyry Cu–Au ore fluids: evidence from silicate and sulfide melt inclusions. Miner Depos 39:845–863

Harms E, Schmincke HU (2000) Volatile composition of the phonolitic Laacher See magma (12,900 yr BP); implications for syn-eruptive degassing of S, F, Cl and H_2O. Contrib Miner Petrol 138:84–98

Harms E, Gardner JE, Schmincke HU (2004) Phase equilibria of the Lower Laacher See tephra (East Eifel, Germany): constraints on pre-eruptive storage conditions of a phonolitic magma reservoir. J Volcanol Geotherm Res 134:135–148

He ZW, Huang F, Yu H, Xiao Y, Wang F, Li Q, Xia Y, Zhang X (2016) A flux-free fusion technique for rapid determination of major and trace elements in silicate rocks by LA-ICP-MS. Geostand Geoanal Res 40:5–21

Jenner FE, O'Neill HSC, Arculus RJ, Mavrogenes JA (2010) The Magnetite Crisis in the Evolution of Arc-related Magmas and the Initial Concentration of Au, Ag and Cu. J Petrol 51:2445–2464

Jouvin D, Weiss DJ, Mason TFM, Bravin MN, Louvat P, Zhao F, Ferec F, Hinsinger P, Benedetti MF (2012) Stable isotopes of Cu and Zn in higher plants: evidence for Cu reduction at the root surface and two conceptual models for isotopic fractionation processes. Environ Sci Technol 46:2652–2660

Jung C, Jung S, Hoffer E, Berndt J (2006) Petrogenesis of Tertiary mafic alkaline magmas in the Hocheifel, Germany. J Petrol 47:1637–1671

Jung S, Pfänder JA, Brauns M, Maas R (2011) Crustal contamination and mantle source characteristics in continental intra-plate volcanic rocks: Pb, Hf and Os isotopes from central European volcanic province basalts. Geochim Cosmochim Acta 75:2664–2683

Kempton PD, Harmon RS, Stosch HG, Hoefs J, Hawkesworth CJ (1988) Open-system O-isotope behaviour and trace element enrichment in the sub-Eifel mantle. Earth Planet Sci Lett 89:273–287

Kimball BE, Mathur R, Dohnalkova AC, Wall AJ, Runkel RL, Brantley SL (2009) Copper isotope fractionation in acid mine drainage. Geochim Cosmochim Acta 73:1247–1263

Lee C-TA, Luffi P, Chin EJ, Bouchet R, Dasgupta R, Morton DM, Le Roux V, Q-z Yin, Jin D (2012) Copper systematics in arc magmas and implications for crust-mantle differentiation. Science 336:64–68

Li WQ, Jackson SE, Pearson NJ, Alard O, Chappell BW (2009) The Cu isotopic signature of granites from the Lachlan Fold Belt, SE Australia. Chem Geol 258:38–49

Li D-D, Liu S-A, Li S-G (2015) Copper isotope fractionation during adsorption onto kaolinite: experimental approach and applications. Chem Geol 396:74–82

Little SH, Sherman DM, Vance D, Hein JR (2014) Molecular controls on Cu and Zn isotopic fractionation in Fe–Mn crusts. Earth Planet Sci Lett 396:213–222

Liu S-A, Teng F-Z, Li S, Wei G-J, Ma J-L, Li D (2014a) Copper and iron isotope fractionation during weathering and pedogenesis: insights from saprolite profiles. Geochim Cosmochim Acta 146:59–75

Liu S-A, Li D, Li S, Teng F-Z, Ke S, He Y, Lu Y (2014b) High-precision copper and iron isotope analysis of igneous rock standards by MC-ICP-MS. J Anal At Spectrom 29:122–133

Liu XC, Xiong XY, Audétat A, Li Y, Song M, Li L, Sun W, Ding X (2014c) Partitioning of copper between olivine, orthopyroxene, clinopyroxene, spinel, garnet and silicate melts at upper mantle conditions. Geochim Cosmochim Acta 125:1–22

Liu S-A, Huang J, Liu J, Wörner G, Yang W, Tang Y-J, Chen Y, Tang L, Zheng J, Li S (2015a) Copper isotopic composition of the silicate Earth. Earth Planet Sci Lett 427:95–103

Liu XC, Xiong XY, Audétat A, Li Y (2015b) Partitioning of Cu between mafic minerals, Fe–Ti oxides and intermediate to felsic melts. Geochim Cosmochim Acta 151:1–22

Lodders K (2003) Solar system abundances and condensation temperatures of the elements. Astrophys J 591:1220–1247

Maher KC, Jackson S, Mountain B (2011) Experimental evaluation of the fluid-mineral fractionation of Cu istotopes at 250 °C and 300 °C. Chem Geol 286:229–239

Maréchal CN, Télouk P, Albarède F (1999) Precise analysis of copper and zinc isotopic compositions by plasma-source mass spectrometry. Chem Geol 156:251–273

Mason TFD, Weiss DJ, Horstwood M, Parrish RR, Russell SS, Mullane E, Coles BJ (2004) High-precision Cu and Zn isotope analysis by plasma source mass spectrometry part 2. Correcting for mass discrimination effects. J Anal At Spectrom 19:218–226

Mathur R, Ruiz J, Titley S, Liermann L, Buss H, Brantley S (2005) Cu isotopic fractionation in the supergene environment with and without bacteria. Geochim Cosmochim Acta 69:5233–5246

Mathur R, Titley S, Barra F, Brantley S, Wilson M, Phillips A, Munizaga F, Maksaev V, Vervoort J, Hart G (2009) Exploration potential of Cu isotope fractionation in porphyry copper deposits. J Geochem Explor 102:1–6

Mathur R, Dendas M, Titley S, Phillips A (2010) Patterns in the copper isotope composition of minerals in porphyry copper deposits in Southwestern United States. Econ Geol 105:1457–1467

Mathur R, Jin L, Prush V, Paul J, Ebersole C, Fornadel A, Williams JZ, Brantley S (2012) Cu isotopes and concentrations during weathering of black shale of the Marcellus Formation, Huntingdon County, Pennsylvania (USA). Chem Geol 304–305:175–184

Mertes H, Schmincke HU (1985) Mafic potassic lavas of the Quaternary West Eifel volcanic field. Contrib Mineral Petrol 89:330–345

Pekala M, Asael D, Butler IB, Matthews A, Rickard D (2011) Experimental study of Cu isotope fractionation during the reaction of aqueous Cu(II) with Fe(II) sulphides at temperatures between 40 and 200 °C. Chem Geol 289:31–38

Pfänder JA, Jung S, Münker C, Stracke A, Mezger K (2012) A possible high Nb/Ta reservoir in the continental lithospheric mantle and consequences on the global Nb budget–Evidence from continental basalts from Central Germany. Geochim Cosmochim Acta 77:232–251

Rempel KU, Liebscher A, Meixner A, Romer RL, Heinrich W (2012) An experimental study of the elemental and isotopic fractionation of copper between aqueous vapour and liquid to 450 °C and 400 bar in the CuCl–NaCl–H_2O and CuCl–NaHS–NaCl–H_2O systems. Geochim Cosmochim Acta 94:199–216

Savage PS, Chen H, Shofner G, Badro J, Moynier F (2013) The copper isotope composition of bulk Earth: a new paradox? Goldshmidt2013 Conferen Abstracts:2142

Savage PS, Harvey J, Moynier F (2014) Copper isotope heterogeneity in the lithospheric mantle. Goldschmidt2014 Conference Abstracts:2192

Savage PS, Moynier F, Chen H, Shofner G, Siebert J, Badro J, Puchtel IS (2015a) Copper isotope evidence for large-scale sulphide fractionation during Earth's differentiation. Geochem Perspect Lett 1:53–64

Savage PS, Moynier F, Harvey J, Burton K (2015b) The behaviour of copper isotopes during igneous processes. AGU 2015 Fall Meeting Abstract: V53B-3137

Schmincke HU (2007) The Quaternary volcanic fields of the east and west Eifel (Germany). In: Ritter JRR, Christensen UR (eds) Mantle plumes; a multidisciplinary approach. Springer, Berlin, pp 241–322

Seo JH, Lee SK, Lee I (2007) Quantum chemical calculations of equilibrium copper (I) isotope fractionations in ore-forming fluids. Chem Geol 243:225–237

Simon AC, Pettke T, Candela PA, Piccoli PM, Heinrich CA (2006) Copper partitioning in a melt–vapor–brine–magnetite–pyrrhotite assemblage. Geochim Cosmochim Acta 70:5583–5600

Toutain J-P, Sonke J, Munoz M, Nonell A, Polvé M, Viers J, Freydier R, Sortino F, Joron J-L, Sumarti S (2008) Evidence for Zn isotopic fractionation at Merapi volcano. Chem Geol 253:74–82

Vance D, Archer C, Bermin J, Perkins J, Statham PJ, Lohan MC, Ellwood MJ, Mills RA (2008) The copper isotope geochemistry of rivers and the oceans. Earth Planet Sci Lett 274:204–213

Wall AJ, Mathur R, Post JE, Heaney PJ (2011) Cu isotope fractionation during bornite dissolution: an in situ X-ray diffraction analysis. Ore Geol Rev 42:62–70

Weinstein C, Moynier F, Wang K, Paniello R, Foriel J, Catalano J, Pichat S (2011) Isotopic fractionation of Cu in plants. Chem Geol 286:266–271

Witt-Eichschen G, Seck HA, Mezger K, Egiins SM, Altherr R (2003) Lithospheric mantle evolution beneath the Eifel (Germany): constraints from Sr–Nd–Pb isotopes and trace element abundances in spinel peridotite and pyroxenite xenoliths. J Petrol 44:1077–1095

Witt-Eickschen G, Kramm U (1998) Evidence for the multiple stage evolution of the subcontinental lithospheric mantle beneath the Eifel (Germany) from pyroxenite and composite pyroxenite/peridotite xenoliths. Contrib Mineral Petrol 131:258–272

Wörner G, Schmincke H-U (1984a) Mineralogical and chemical zonation of the Laacher See tephra sequence (East Eifel, W. Germany). J Petrol 25:805–835

Wörner G, Schmincke H-U (1984b) Petrogenesis of the zoned Laacher See tephra. J Petrol 25:836–851

Wörner G, Wright TL (1984) Evidence for magma mixing within the Laacher See magma chamber (East Eifel, Germany). J Volcanol Geotherm Res 22:301–327

Wörner G, Schmincke H-U, Schreyer W (1982) Crustal xenoliths from the Quaternary Wehr volcano (East Eifel). Neues Jahrbuch fuer Mineralogie Abhandlungen 1:29–55

Wörner G, Beusen J-M, Duchateau N, Gijbels R, Schmincke H-U (1983) Trace element abundances and mineral/melt distribution coefficients in phonolites from the Laacher See Volcano (Germany). Contrib Mineral Petrol 84:152–173

Wörner G, Staudigel H, Zindler A (1985) Isotopic constraints on open system evolution of the Laacher See magma chamber (Eifel, West Germany). Earth Planet Sci Lett 75:37–49

Wörner G, Zindler A, Staudigel H, Schmincke H-U (1986) Sr, Nd, and Pb isotope geochemistry of Tertiary and Quaternary alkaline volcanics from West Germany. Earth Planet Sci Lett 79:107–119

Wörner G, Harmon RS, Hoefs J (1987) Stable isotope relations in an open magma system, Laacher See, Eifel (FRG). Contrib Mineral Petrol 95:343–349

Zhu XK, Guo Y, Williams RJP, O'Nions RK, Matthews A, Belshaw NS, Canters GW, de Waal EC, Weser U, Burgess BK, Salvato B (2002) Mass fractionation processes of transition metal isotopes. Earth Planet Sci Lett 200:47–62